

Exact real time dynamics with free fermions in disguise

István Vona,^{1,2} Márton Mestyán,¹ and Balázs Pozsgay¹

¹MTA-ELTE “Momentum” Integrable Quantum Dynamics Research Group,
ELTE Eötvös Loránd University, Budapest, Hungary

²Holographic Quantum Field Theory Research Group,
HUN-REN Wigner Research Centre for Physics, Budapest, Hungary

We consider quantum spin chains with a hidden free fermionic structure, distinct from the Jordan-Wigner transformation and its generalizations. We express selected local operators with the hidden fermions. This way we can exactly solve the real time dynamics in various physical scenarios, including the computation of selected dynamical two point functions, in continuous or discrete time. In the latter case we build a quantum circuit that can be implemented on a quantum computer. With this we extend the family of classically simulable quantum many-body processes.

I. INTRODUCTION

Free fermions play an important role in multiple areas of theoretical physics, due to their exact solvability and the simplicity of the computations with them. The two-dimensional classical Ising model is solvable by free fermions [1], just like many one dimensional quantum spin chains, such as the Ising chain or the XX model [2]. The free fermionic Kitaev chain [3] is an important candidate for fault tolerant quantum computing. In two dimensions the honeycomb lattice model is a free fermionic system that hosts anyons [4]. Free fermions are important also in quantum information theory: quantum circuits based on the so-called matchgates are free fermionic, and they enable classical simulability of quantum processes [5–7]. Free fermions also appear in the tensor network models of the holographic principle, where they lead to an efficient contraction of the network [8].

Given their importance it is natural to ask: What is the widest class of physically meaningful models which can be solved by free fermions? How can we construct free fermionic operators in systems that are inherently bosonic? And what is the true computational advantage of the free fermions?

In quantum spin chains fermions can be constructed using the Jordan-Wigner (JW) transformation [9] (for generalizations see [10–15]). However, the JW transformation does not encompass all possibilities. In the last couple of years a number of models have been found which can be solved by hidden free fermionic structures [16–21] (for earlier examples see [22–24]). These models typically involve 4-body or higher interactions when expressed using the JW fermions; but the Hamiltonian can be diagonalized by the hidden fermionic operators. These are highly non-local in the original spin operators, but also in the JW fermions. The solution of hidden-fermion models is also different from a generalized JW transformation in that it is not possible to express every local term in the Hamiltonian individually as a bilinear in the hidden fermions [13, 14, 19]. Previous works focused on computing the spectrum and the ground state properties of such models [25–29] but the practical advantage of the free fermionic structures has not yet been

demonstrated beyond the computation of the spectrum.

In this work we establish contact with local physics, focusing on the “free fermions in disguise” (FFD) model of Fendley [16]. For the first time we express selected local operators using the hidden fermions, thereby partially solving the “inverse problem”. Afterwards we treat the real time dynamics analytically in various scenarios. Our work is the first one to compute such analytic results, and with this we demonstrate the practical usefulness of hidden free fermions.

Besides Hamiltonian dynamics we also consider discrete time evolution in quantum circuits with special geometries, compatible with the FFD model. These circuits can be realized in present-day quantum computers. With this we demonstrate that free fermions in disguise lead to classically simulable quantum processes and this could be used for benchmarking quantum computers.

II. MODEL

We consider one dimensional quantum spin chains and quantum circuits which are built on selected representations of an abstract algebra. We call it the FFD algebra. It is defined by the generators h_j , $j = 1, 2, \dots, M$ which satisfy $h_j^2 = 1$, $h_j = h_j^\dagger$ and the commutation relations

$$\begin{aligned} \{h_j, h_{j+1}\} &= \{h_j, h_{j+2}\} = 0 \\ [h_j, h_k] &= 0, \quad |j - k| > 2. \end{aligned} \tag{1}$$

These relations are understood without periodicity in the indices, therefore the algebra always describes a system with open boundaries.

We consider a family of models defined by the Hamiltonians

$$H = \sum_{j=1}^M b_j h_j \tag{2}$$

where $b_j \in \mathbb{R}$ are arbitrary coupling constants. We specify a representation of the abstract algebra on a spin 1/2-chain of length $L = M$. The concrete operators are given by $h_1 = X_1$, $h_2 = Z_1 X_2$, and

$$h_j = Z_{j-2} Z_{j-1} X_j, \quad j \geq 3. \tag{3}$$

Here and below X_j , Y_j and Z_j stand for the Pauli matrices acting on site j of the spin chain. Other representations were treated in [16, 30]. The results to be presented below do not depend on the concrete representation: different representations only change certain degeneracies, but the techniques we develop are not affected by this.

III. JORDAN-WIGNER SOLVABILITY

Introducing standard Jordan-Wigner fermions as

$$\chi_{2k-1} = Z_k \prod_{j=1}^{k-1} X_j, \quad \chi_{2k} = Y_k \prod_{j=1}^{k-1} X_j \quad (4)$$

we see that the h_j are quartic in the fermions

$$h_j = -\chi_{2j-4}\chi_{2j-3}\chi_{2j-1}\chi_{2j}, \quad (5)$$

for $j \geq 3$. One might wonder whether the model is solvable by a generalized Jordan-Wigner transformation. It was proven in [19] that this is not possible: there are no Majorana fermions $\tilde{\chi}_a$ such that every operator h_j is expressed as a product of two Majorana fermions [13, 14] like

$$h_j = i\tilde{\chi}_{a_j}\tilde{\chi}_{b_j}, \quad \forall j, \quad (6)$$

for a given mapping from j to the pairs of indices a_j, b_j .

However, the parameters of the model can be specified so that it becomes Jordan-Wigner solvable. For example, if we set every third b_j coupling to zero, then we can introduce a re-labeling for the remaining terms as

$$b_{3j} = 0 : \quad \tilde{h}_{2k-1} = h_{3k-2}, \quad \tilde{h}_{2k} = h_{3k-1}, \quad (7)$$

for $j = 1, 2, \dots, \lfloor M/3 \rfloor$ and $k = 1, 2, \dots, \lfloor M/3 + 1/2 \rfloor$. In a similar way we can switch off every second coupling and define the new set of Hamiltonian densities as

$$b_{2j} = 0 : \quad \tilde{h}_k = h_{2k-1}, \quad (8)$$

with $j = 1, 2, \dots, \lfloor M/2 \rfloor$ and $k = 1, 2, \dots, \lfloor M/2 \rfloor$. We find that in both cases these operators satisfy the reduced algebra

$$\{\tilde{h}_j, \tilde{h}_{j+1}\} = 0, \quad [\tilde{h}_j, \tilde{h}_k] = 0 \text{ for } |j - k| > 1. \quad (9)$$

These relations describe the terms in the Hamiltonian in the quantum Ising chain, and the model becomes Jordan-Wigner solvable [10, 13, 14, 31]. In this special case all our results below become identical to those obtained by the standard methods; detailed comparisons will be presented elsewhere. In the following we consider generic choices of the parameters b_j .

IV. SOLUTION

The model possesses a family of extensive conserved charges. They are given by the logarithmic derivatives

of a transfer matrix $T_M(u)$, which can be defined via the recursion relation

$$T_M(u) = T_{M-1}(u) - ub_M h_M T_{M-3}(u), \quad (10)$$

with the initial conditions $T_M(u) = 1$ for $M \leq 0$. The order of $T_M(u)$ in u is $S = [(M+2)/3]$. The Hamiltonian is obtained as $H = -\partial_u T_M(u)|_{u=0}$. The transfer matrices satisfy $[T_M(u), T_M(v)] = 0$, therefore they also commute with the Hamiltonian. Furthermore, they satisfy an inversion relation

$$T_M(u)T_M(-u) = P_M(u^2) \cdot \mathbb{1}. \quad (11)$$

Here $P_M(x)$ is a polynomial of order S , which is given by the recursion relation

$$P_M(x) = P_{M-1}(x) - xb_M^2 P_{M-3}(x) \quad (12)$$

where $P_{-2}(x) \equiv P_{-1}(x) \equiv P_0(x) \equiv -1$. These polynomials and their generalizations were studied also in the mathematical literature [32, 33]; the values $P_M(-1)$ for $b_j \equiv 1$ are known as Narayana's cows sequence [34, 35].

It was proven in [16] that the model possesses a hidden free fermionic structure. There exist operators Ψ_k and $\Psi_{-k} \equiv \Psi_k^\dagger$, $k = 1, 2, \dots, S$, such that

$$\{\Psi_k, \Psi_\ell\} = \{\Psi_{-k}, \Psi_{-\ell}\} = 0, \quad \{\Psi_k, \Psi_{-\ell}\} = \delta_{k,\ell}, \quad (13)$$

which diagonalize the Hamiltonian via

$$H = \sum_{k=1}^S \varepsilon_k [\Psi_k, \Psi_{-k}]. \quad (14)$$

Here the ε_k are interpreted as (half of the) single particle energies associated with the eigenmodes. They are given by $\varepsilon_k = (u_k)^{-1}$, with u_k being the roots of a polynomial $P_M(u^2)$.

It follows from (14) that the energy levels of the Hamiltonian are given by

$$E = \sum_{k=1}^S \pm \varepsilon_k. \quad (15)$$

There are only $S = [(M+2)/3]$ fermionic eigenmodes for a size M of the algebra, and this is the same number for all faithful representations. This implies that each level is degenerate with the same level of degeneracy which increases exponentially with M . The size of the degeneracies depends on the representation, because the length L of the spin chain for a given M can vary. In our case $L = M$, therefore the size of the degenerate sectors is 2^{M-S} . For other representations see [16, 30].

The physical properties of the model depend on the choice of the coupling constants b_j . It is natural to choose staggered couplings with period 3:

$$b_{3j} = \alpha, \quad b_{3j+1} = \beta, \quad b_{3j+2} = \gamma. \quad (16)$$

The resulting phase diagram was studied in [16]. The set of the energy levels has a gap for generic α, β, γ , but there are gapless lines in the phase diagram, and the homogeneous choice $\alpha = \beta = \gamma$ corresponds to a special multi-critical point. We refer to [16] for more details.

V. FERMIONS

The construction of the fermionic operators is based on the so-called edge operator χ_0 . This is a Hermitian operator satisfying $\chi_0^2 = 1$, $\{\chi_0, h_1\} = 0$ and $[\chi_0, h_j] = 0$ for $j > 1$. For certain values of M we can choose χ_0 to be a member of the FFD algebra [30], but it can also be an extra element. In the representation (3) we can choose $\chi_0 = Z_1$.

The explicit formula for the fermionic operators is [16]

$$\Psi_{\pm k} = \frac{1}{\mathcal{N}_k} T_M(\mp u_k) \chi_0 T_M(\pm u_k), \quad (17)$$

where \mathcal{N}_k is a known normalization factor, see (B8). The Ψ_k depend on the choice of the auxiliary element χ_0 ; this reflects a gauge freedom arising from the degeneracies [16, 30]. However, correlation functions of the elements of the FFD algebra are independent of this choice.

VI. THE INVERSE PROBLEM

In order to compute correlation functions one needs to express local operators using the hidden fermions. In Jordan-Wigner solvable models with periodic boundary conditions the fermionic eigenmodes are Fourier transforms of local fermionic operators, and the inverse problem is solved by the inverse Fourier transform. However, the situation is more complicated in the FFD algebra, because (17) is more involved than a Fourier transform. Furthermore, the FFD algebra has only S fermionic eigenmodes for a given size M , therefore the inverse problem can not be fully solved, and we can only expect solutions for selected local operators.

Our strategy is to expand χ_0 as a linear combination of the fermionic operators as

$$\chi_0 = \sum_{j=-S, j \neq 0}^S C_j \Psi_j, \quad (18)$$

and to compute the C_j . Afterwards we construct a family of operators which are bilinears in the fermions. Using the results of [16] we show in Appendix B that the coefficients are

$$C_j = C_{-j} = \sqrt{\frac{P_{M \setminus 1}(u_j^2)}{-u_j^2 P'_M(u_j^2)}}, \quad (19)$$

where $P_{M \setminus 1}(x)$ stands for a polynomial which is obtained analogous to $P_M(x)$ but with the substitution $b_1 = 0$ and the prime in P'_M denotes differentiation with respect to its argument.

It remains to be checked whether the expansion above is complete. We performed numerical tests for small values of M and discovered that for $M = 3k$ and $M = 3k+2$ the model possesses a Majorana zero mode as well. This

is described by a Hermitian operator Ψ_0 with the properties $(\Psi_0)^2 = 1$, $[H, \Psi_0] = 0$ and $\{\Psi_0, \Psi_k\} = \{\Psi_0, \Psi_{-k}\} = 0$ for $k = 1, 2, \dots, S$. The zero mode is not a boundary mode: it is de-localized as the other fermionic modes - see (B5) and (B6).

If we add the zero mode as

$$\chi_0 = \sum_{j=-S}^S C_j \Psi_j, \quad C_0 = \begin{cases} 0 & M \in 3\mathbb{N} + 1, \\ \prod_{k=1}^S \frac{u_k}{\hat{u}_k} & \text{else,} \end{cases} \quad (20)$$

where $\hat{u}_k > 0$ are the roots $P_{M \setminus 1}(\hat{u}_k^2) = 0$, then numerical tests and an analytic proof show in Appendix B that the expansion is complete, and we solved the inverse problem of χ_0 .

We now express other operators using the fermions, by employing the FFD algebra together with (14). A simple way is to construct a series of operators o_j via the recursion

$$o_j = \frac{1}{2} [H, o_{j-1}], \quad (21)$$

together with the initial condition $o_0 = \chi_0$. This can be seen as a Krylov basis in operator space. Such an approach was already used in [20] to establish the existence of hidden free fermions in related models. Here we use it simply to find the first few examples of composite local operators, which take a simple expression in terms of the fermionic eigenmodes.

H is bilinear in the fermions, while $o_0 = \chi_0$ is linear, therefore every o_j is also linear in the fermions. In the FFD algebra representation every o_j includes a factor of χ_0 . Having found the o_j , we construct the products $o_j o_k$ and take their linear combinations, to obtain a family of local operators that are bi-linear in the fermions. It is crucial that χ_0 drops out from every such product.

For the first element we find $o_1 = b_1 h_1 \chi_0$. Taking the product $o_1 \chi_0 = b_1 h_1$ we compute h_1 as a bi-linear expression in the fermions. It follows from (14), (20), and the fermionic algebra that

$$h_1 = b_1^{-1} \sum_{j, k=-S}^S \varepsilon_j C_j C_k \Psi_j \Psi_k. \quad (22)$$

Going further we find $o_2 = ((b_2 h_2 + b_3 h_3) b_1 h_1 + b_1^2) \chi_0$, and using this result we can express the combination $b_2 h_2 + b_3 h_3$ as a bi-linear in the fermions. However, we did not find a way to express h_2 and/or h_3 individually using the fermions. Afterwards the next simplest operator for which a bi-linear expression is found is a linear combination of h_4 , h_5 and $h_2 h_3 h_5$ as discussed in Appendix C. Our method expresses increasingly complicated local operators using the fermions. At present we do not have a full classification as to which local operator is bi-linear, or perhaps of higher order in the hidden fermions.

VII. DYNAMICS

We compute infinite temperature two-point functions of operators localized around the boundary. Our main example is the self-correlator of the boundary energy density

$$D(t) = \langle h_1(t)h_1(0) \rangle \equiv \text{Tr}(h_1 e^{-iHt} h_1 e^{iHt})/\text{Tr}(\mathbb{1}). \quad (23)$$

This correlation function can be expressed as

$$D(t) = \frac{1}{4b_1^2} \left((\dot{B}(t))^2 - B(t)\ddot{B}(t) \right), \quad (24)$$

where the dot means the time-derivative and the function $B(t)$ is the correlator of the edge operator itself

$$B(t) = \langle \chi_0(t)\chi_0(0) \rangle. \quad (25)$$

As explained in Appendix D formula (24) is the consequence of the fact that the time-evolved Krylov-basis elements $o_j(t)$ can be generated by repeatedly differentiating $\chi_0(t)$ w.r.t t , and also Wick's theorem and the time-translation invariance of the correlators.

The time evolution of the fermionic modes is given by $\Psi_{\pm k}(t) = e^{\pm 2i\varepsilon_k t} \Psi_{\pm k}$, and a standard computation yields

$$B(t) = \sum_{k=0}^S C_k^2 \cos(\theta_k), \quad \theta_k \equiv 2\varepsilon_k t \quad (26)$$

while substituting it into (24) gives

$$D(t) = \sum_{k,\ell=0}^S \frac{C_k^2 C_\ell^2}{4b_1^2} \sum_{\sigma=\pm} (\varepsilon_k - \sigma \varepsilon_\ell)^2 \cos(\theta_k + \sigma \theta_\ell). \quad (27)$$

Note that a typical free-fermionic calculation starting out directly from formula (22) leads to the same result. We introduced the extra step and $B(t)$ as the latter is a good building block for obtaining correlators of the more complicated local operators discussed in Section VI, and it was also simpler to analyze this function in the thermodynamical limit as explained in Section VIII.

VIII. RESULTS

The above formula can be evaluated in polynomial time for every M and arbitrary set of coupling constants. It is natural to consider parameters with a period 3 staggering, in which case the model displays a rich phase diagram [16]. We numerically evaluated the correlation function $D(t)$ for different values of M and various choices of the staggered parameters. We found that the correlation function can show various types of behaviour: it can decay to zero with some power law, it can converge to a non-zero value, and it can also show persistent oscillations around a non-zero value. Similar variation of dynamical boundary correlations was observed earlier in

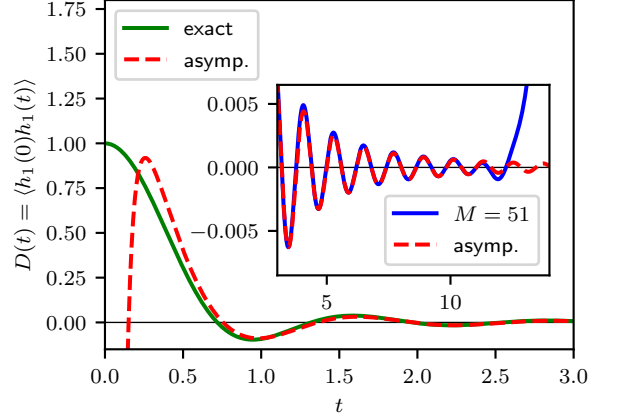


Figure 1. The boundary correlation function $D(t)$ in the thermodynamic limit $M \rightarrow \infty$, plotted against the asymptotic formula (30). The inset shows a comparison for finite M .

standard free fermionic systems [36–38]; a full analysis of the behaviour of $D(t)$ will be presented elsewhere.

Here we focus on the completely homogeneous case with $b_k = 1$ for $k = 1, \dots, M$. This is a multi-critical point in the phase diagram, where the energy gap (determined by the smallest ε_k) scales as M^{-z} with the unusual exponent $z = 3/2$. We computed a closed form result for $B(t)$ in the $M \rightarrow \infty$ limit, by transforming the finite sum into a contour integral. Our final result reads

$$B(t) = \int_0^\pi dp C^2(p) \cos(2t\varepsilon(p)), \quad (28)$$

where p is a momentum-like variable, and $\varepsilon(p)$ and $C(p)$ are known functions, defined in (E1) and (E16) respectively. We also showed that $B(t)$ can be expressed alternatively using the generalized hypergeometric function ${}_pF_q(a; b; z)$ as

$$B(t) = {}_2F_3 \left(\frac{1}{3}, \frac{2}{3}; \frac{1}{2}, 1, \frac{3}{2}; -\frac{27t^2}{4} \right), \quad (29)$$

see also (E17). The correlation function $D(t)$ is computed afterwards via (24).

The long-time asymptotics of $D(t)$ looks as

$$D(t) \approx \alpha \frac{\sin(3\sqrt{3}t + 3\pi/4)}{t^{13/6}}, \quad (30)$$

where α is a known constant from (F6). The unusual scaling exponent 13/6 arises from the combination of two asymptotic contributions to $B(t)$, see (F5).

In Figure 1 we plotted the function $D(t)$ for finite M and also in the $M \rightarrow \infty$ limit, together with the asymptotic form given above. More details about the numerical computations are presented in Appendix I.

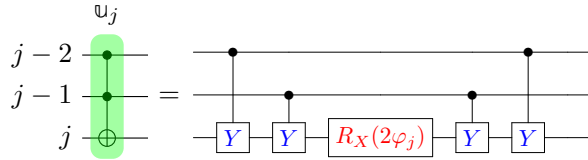


Figure 2. Quantum circuit of the 3-site operator u_j

IX. QUANTUM CIRCUIT

Let us now return to finite M and consider discrete time evolution in a quantum circuit. Our aim is to derive a circuit that can be realized in present-day quantum computers, and which is compatible with the hidden free fermions [30].

The transfer matrix $T_M(u)$ admits a factorization, which yields a unitary quantum circuit if u is purely imaginary [16, 30]. This way we obtain a unitary matrix $\mathcal{V}(\delta)$ parametrized by $\delta \in \mathbb{R}$, given by

$$\mathcal{V}(\delta) = G \cdot G^T, \quad G = u_1 u_2 \cdots u_{M-1} u_M, \quad (31)$$

where $u_j = e^{i\varphi_j h_j}$ are local unitary gates with the angles φ_j given by the recursion

$$\tan(2\varphi_j) = -\delta b_j \cos(2\varphi_{j-1}) \cos(2\varphi_{j-2}) \quad (32)$$

together with $\varphi_0 = \varphi_{-1} = 0$. For small values of δ we get $\mathcal{V}(\delta) \approx 1 - i\delta H$, therefore $\mathcal{V}(\delta)$ can be seen as a “free fermionic Trotterization” of the FFD Hamiltonian, with δ playing the role of the discretization time step. Note that the circuit is free fermionic for any choice of the φ_j -s, as the b_j parameters can be chosen arbitrarily.

We choose the circuit $\mathcal{V}(\delta)$ to generate discrete time evolution. We define dynamical two-point functions as

$$\mathcal{D}(\delta, N) = \text{Tr}(h_1 \mathcal{V}(\delta)^N h_1 \mathcal{V}(-\delta)^N) / \text{Tr}(\mathbb{1}). \quad (33)$$

In the original work [16] the factorization of the form (31) was derived for the transfer matrix, but it is the novelty of this work and the parallel work [30] to use this factorization to build unitary circuits with local gates. We use the formulas of [16] specialized to the unitary case, we extend them with our solution of the inverse problem, and this way we compute the answer for $\mathcal{D}(\delta, N)$. We obtain formally the same formula as in (27), but now with the phases $\theta_k = 2N \text{atan}(\varepsilon_k \delta)$, for details see Appendix G.

In the representation (3) the local gates u_j are controlled unitaries in the Z -basis, and they can be decomposed into 4 CY gates and 1 single qubit rotation as depicted in Figure 2, for details see Appendix H and [39]. The complete circuit geometry of (31) is shown in Figure 3. Therefore the circuit $\mathcal{V}(\delta)$ can be implemented on a quantum computer.

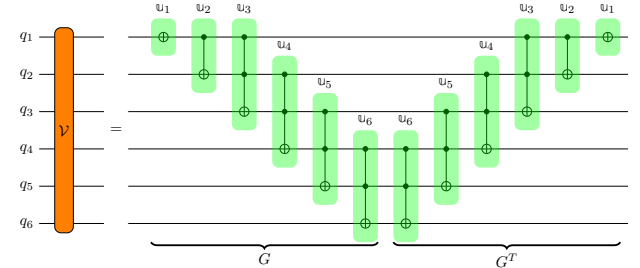


Figure 3. The staircase-like structure of \mathcal{V} for $M = 6$ qubits

X. DISCUSSION

We used the hidden free fermionic structure to compute the time evolution of selected physical observables. All the problems considered here can be solved in polynomial time in M , including finding the roots u_k and evaluating the summations for the observables. This means that we can classically simulate the corresponding quantum many-body processes.

Our framework should be compared to circuits made up of matchgates [5–7], which are two-site gates whose logarithm is bi-linear in the Jordan-Wigner fermions. Any product of the matchgates is still free fermionic; the only requirement is that each gate should act on two neighbouring sites.

By contrast, in our framework the gates in the circuit need to be arranged in a special way to preserve the hidden free fermionic property. Here we treated only one arrangement, while other circuit arrangements are explored in [30]. Currently it is not known what is the most general class of circuits compatible with the free fermions, and this is a direction for future research.

There is another limitation regarding the set of operators whose correlators can be calculated - in the efficient way outlined in the paper - on the basis of the hidden fermionic modes. We presented examples in Section VI, but currently we do not have a full characterization of the allowed operators and their locality properties. We hope to return to this question in future work.

In this work we only treated one specific model, namely the original model of [16]. However, we expect that our techniques can be applied also to the more general class of models with hidden free fermions, treated in [19, 20] (see also [21]).

ACKNOWLEDGMENTS

We are thankful to János Asbóth, Paul Fendley, Esperanza Lopez, Lorenzo Piroli, Roberto Ruiz, German Sierra, Alejandro Sopena, Eric Vernier for stimulating discussions. We also benefitted from the workshop “Exactly Solved Models and Quantum Computing” organized at the Lorentz Center, Leiden, The Netherlands, in March 2024. The authors were supported

by the Hungarian National Research, Development and Innovation Office, NKFIH Grant No. K-145904 and B.P. was supported by the NKFIH excellence grant TKP2021_NKTA_64.

Appendix A: Basic properties of the transfer matrix

Here we collect a few basic properties of the transfer matrix $T_M(u)$ and the associated polynomials [16]. In the main text the operator $T_M(u)$ is defined via the recursion relation (10), which can be evaluated in a straightforward way. Alternatively, we can also express it as the power series

$$T_M(u) = \sum_{\alpha=0}^S (-u)^\alpha Q^{(\alpha)}, \quad (\text{A1})$$

where $Q^{(\alpha)}$ is a set of commuting non-local charges, together with $Q^{(0)} = \mathbb{1}$. Introducing $H_k = b_k h_k$ the explicit formula for $Q^{(\alpha)}$ is given by

$$Q^{(\alpha)} = \sum_{j_{k+1} > j_k + 2} H_{j_1} H_{j_2} \dots H_{j_\alpha}. \quad (\text{A2})$$

Here the summation is over those subsets of indices $(j_1, j_2, \dots, j_\alpha)$ where every pair of operators H_{j_k}, H_{j_ℓ} commutes, leading to the condition $j_{k+1} > j_k + 2$. The equivalence between the two expressions for $T_M(u)$ can be proven by induction over M .

An important property of the transfer matrix is the inversion relation (11). The polynomials $P_M(x)$ that arise there are defined by the recursive relations (12) or alternatively via

$$P_M(x) = \sum_{\alpha=0}^S (-x)^\alpha \sum_{j_{k+1} > j_k + 2} (b_{j_1} b_{j_2} \dots b_{j_\alpha})^2. \quad (\text{A3})$$

For completeness we note that $P_M(x)$ can be interpreted as a weighted *independence polynomial* of the so-called frustration graph of the Hamiltonian, for details see [20].

In the computations below we also use the restricted transfer matrix $T_{M \setminus 1}(u)$, which is obtained from $T_M(u)$ simply by setting $b_1 = 0$. It can be also understood as the transfer matrix of the chain of length $M-1$ with coupling constants (b_2, b_3, \dots, b_M) . The associated polynomial is denoted by $P_{M \setminus 1}(u)$.

Appendix B: Decomposition of the edge operator

Here we show the edge operators' expansion via the fermionic modes and discuss the completeness of said expression.

Let us consider the operator valued function

$$\phi_M(u) = -\frac{1}{u} \left(\frac{P_M(u^2) \chi_0 + T_M(-u) \chi_0 T_M(u)}{2P_M(u^2)} \right) \quad (\text{B1})$$

and its integral over the double keyhole contour depicted in Figure 4. We use this contour integral as an auxiliary object to find the desired expansion of χ_0 in terms of the fermionic operators.

The transfer matrix and thus the numerator of $\phi_M(u)$ are both polynomials in u . Therefore the singularities of $\phi_M(u)$ on the complex u plane consist only of the poles coming from the zeros $u = \pm u_j$ of

$$P_M(u^2) = \prod_{l=1}^S (1 - u^2/u_l^2), \quad (\text{B2})$$

and the simple pole at $u = 0$ introduced by the $1/u$ factor. The set of zeros is known to be non-degenerate [18] and therefore the other poles are simple as well. The closed contour then divides the complex plane into two regions. The residue theorem inside gives simply $-\text{Res}_{u=0} \phi_M(u) = \chi_0$, while for the outside region it picks up the contributions coming from the rest of the poles

$$\chi_0 \stackrel{\text{inside}}{=} \frac{1}{2\pi i} \int_C du \phi_M(u) \stackrel{\text{outside}}{=} \sum_{j=-S}^S \text{Res}_{u=u_j} \phi_M(u) \quad (\text{B3})$$

including the residue at infinity (picked up by the large circle part of the contour). Here we adopted the shorthand notation where $u_{-j} \equiv -u_j$ for $j = 1, 2, \dots, S$ and formally $u_0 \equiv \infty$. When evaluated individually, these terms are proportional to the $j \neq 0$ fermionic modes

$$\text{Res}_{u=u_j} \phi_M(u) = \frac{T_M(-u_j) \chi_0 T_M(u_j)}{-4u_j^2 P'_M(u_j^2)} = \frac{\mathcal{N}_j \Psi_j}{-4u_j^2 P'_M(u_j^2)}, \quad (\text{B4})$$

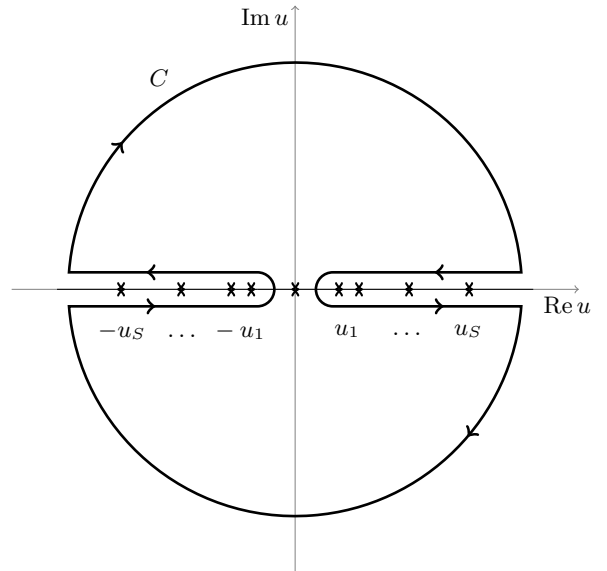


Figure 4. Contour integral to pick up the residues of the poles in the operator $\phi_M(u)$ at $u = \pm u_j$, $j = 1, \dots, S$ and the residue at infinity. On the other hand the contour encloses the pole at $u = 0$ whose residue is χ_0 itself.

while the residue at infinity for $j = 0$ gives

$$\mathcal{Q} \equiv \operatorname{Res}_{u=\infty} \phi_M(u) \stackrel{v \equiv 1/u}{=} \operatorname{Res}_{v=0} \left(-\frac{1}{v^2} \phi_M(v^{-1}) \right) = \lim_{u \rightarrow \infty} \mathcal{Q}_u, \quad (\text{B5})$$

where we introduced

$$\mathcal{Q}_u \equiv -u\phi_M(u) = \frac{1}{2} \left(\chi_0 + \frac{T_M(-u)\chi_0 T_M(u)}{P_M(u^2)} \right). \quad (\text{B6})$$

This gives yet another potentially finite contribution that we need to analyze. In [16] it was derived that

$$\{\Psi_j, \chi_0\} = \frac{4P_{M \setminus 1}(u_j^2)}{\mathcal{N}_j} \mathbb{1}, \quad (\text{B7})$$

together with the normalization of the fermions

$$\mathcal{N}_k = 4\sqrt{-u_k^2 P'_M(u_k^2) P_{M \setminus 1}(u_k^2)}, \quad (\text{B8})$$

where $P_{M \setminus 1}(u_k^2)$ is the restricted polynomial introduced above. The coefficients on the r.h.s. of (B4) and (B7) are exactly the same for $j \neq 0$:

$$C_{\pm j} = \frac{4P_{M \setminus 1}(u_j^2)}{\mathcal{N}_j} = \frac{\mathcal{N}_j}{-4u_j^2 P'_M(u_j^2)} = \sqrt{\frac{P_{M \setminus 1}(u_j^2)}{-u_j^2 P'_M(u_j^2)}}. \quad (\text{B9})$$

If we substitute the decomposition (B3) of χ_0 into (B7) and use the anticommutation relations of the Ψ_j , then they anticommute with the object \mathcal{Q} in (B5) :

$$\{\mathcal{Q}, \Psi_{\pm j}\} = 0, \quad j = 1, 2, \dots, S. \quad (\text{B10})$$

Furthermore,

$$[H, \mathcal{Q}] = 0 \quad (\text{B11})$$

follows by the mode-expansion of the Hamiltonian (14).

There is one more property of $\mathcal{Q} = \lim_{u \rightarrow \infty} \mathcal{Q}_u$ we ought to show. Using the recursion relation (10) and the commutation/anticommutation relations of χ_0 with h_1 and the rest of the h_m -s one can easily show that $\{T_M(u), \chi_0\} = 2T_{M \setminus 1}(u)\chi_0$ which then may be used to move χ_0 in \mathcal{Q}_u at the end (or start) of the expression:

$$\mathcal{Q}_u = \frac{T_M(-u)T_{M \setminus 1}(u)}{P_M(u^2)} \chi_0 = \chi_0 \frac{T_{M \setminus 1}(-u)T_M(u)}{P_M(u^2)}. \quad (\text{B12})$$

Now in the $u \rightarrow \infty$ limit the expressions above vanish, if the cumulative order of the transfer matrices in the numerator is smaller than that of $P_M(u^2)$. This can only happen if the order S' of $T_{M \setminus 1}(u)$ is smaller than S :

$$S' = \left[\frac{(M-1)+2}{3} \right] < \left[\frac{M+2}{3} \right] = S, \quad (\text{B13})$$

which happens only if $M \in 3\mathbb{N} + 1$. Otherwise, by multiplying the two forms of (B12) together we have

$$\mathcal{Q}^2 = \lim_{u \rightarrow \infty} \mathcal{Q}_u^2 = \lim_{u \rightarrow \infty} \frac{P_{M \setminus 1}(u^2)}{P_M(u^2)} \cdot \mathbb{1}, \quad (\text{B14})$$

that is, \mathcal{Q} squares to the identity, up to normalization. By looking at the properties above we can conclude that \mathcal{Q} is proportional to a Majorana zero mode Ψ_0

$$\mathcal{Q} = C_0 \Psi_0 \quad (\text{B15})$$

with energy $\varepsilon_0 = 1/u_0 = 0$, that exists only if $M \notin 3\mathbb{N} + 1$. If we also choose its normalisation such that $\{\Psi_0, \Psi_0\} = 2$, our full set of fermionic anticommutation relations will look as

$$\{\Psi_k, \Psi_{k'}\} = 2^{\delta_{k,0}} \delta_{k+k'} \mathbb{1}, \quad (\text{B16})$$

with $k, k' = -S, \dots, 0, \dots, S$. Then, by (B14), the constant C_0 can be fixed to

$$C_0 = \sqrt{\lim_{u \rightarrow \infty} \frac{P_{M \setminus 1}(u^2)}{P_M(u^2)}} = \begin{cases} 0 & M \in 3\mathbb{N} + 1 \\ \prod_{k=1}^S \frac{u_k}{\hat{u}_k} & \text{else,} \end{cases} \quad (\text{B17})$$

where \hat{u}_k are the (positive) roots of the polynomial $P_{M \setminus 1}(u^2)$. Finally, the decomposition of the edge operators is found as

$$\chi_0 = \sum_{j=-S}^S C_j \Psi_j, \quad (\text{B18})$$

with the coefficients defined in (B9) and (B17).

Appendix C: Krylov basis in operator space

Here we give more details about the computation of local operators that are bi-linear in the fermions. The operator space Krylov basis is defined via

$$o_j = \frac{1}{2} [H, o_{j-1}], \quad (\text{C1})$$

with the initial condition $o_0 = \chi_0$. Using the expansion (B18) we find that

$$o_j = \sum_{k=-S}^S (\varepsilon_k)^j C_k \Psi_k, \quad (\text{C2})$$

where it is understood that $\varepsilon_{-k} \equiv -\varepsilon_k$.

For the first few elements in the Krylov basis we find

$$\begin{aligned} o_0 &= \chi_0 \\ o_1 &= H_1 \chi_0 \\ o_2 &= [(H_2 + H_3)H_1 + b_1^2] \chi_0 \\ o_3 &= (H_4 H_2 + H_4 H_3 + H_5 H_3 + b_1^2 + b_2^2 + b_3^2) H_1 \chi_0, \end{aligned} \quad (\text{C3})$$

where we used the notation $H_j \equiv b_j h_j$ as in Section A. Taking products of the o_j and their linear combinations we obtain operators that are bi-linear in the fermions. For example we find

$$(o_0 - b_1^{-2} o_2) o_1 = H_2 + H_3. \quad (\text{C4})$$

This will give the expansion

$$H_2 + H_3 = \sum_{j,k=-S}^S (1 - b_1^{-2} \varepsilon_j^2) \varepsilon_k C_j C_k \Psi_j \Psi_k. \quad (\text{C5})$$

A further relatively simple combination is

$$\begin{aligned} (o_0 - b_1^{-2} o_2)(o_3 - (b_1^2 + b_2^2 + b_3^2) o_1) \\ = (b_2^2 + b_3^2) H_4 + b_3^2 H_5 + H_2 H_3 H_5. \end{aligned} \quad (\text{C6})$$

This operator is expanded as

$$\sum_{j,k=-S}^S (1 - b_1^{-2} \varepsilon_j^2) \varepsilon_k (\varepsilon_k^2 - (b_1^2 + b_2^2 + b_3^2)) C_j C_k \Psi_j \Psi_k. \quad (\text{C7})$$

It is clear from these computations that every operator product $o_j o_k$ is bi-linear in the fermions, and they can be expressed alternatively as local operator products in the h_j . Furthermore, we could also consider quartic and higher products in the o_j . We expect that certain combinations of h_j can be expressed as simple polynomials in the o_j , but we do not have a prescription to find the simplest such cases.

Appendix D: Free fermionic correlators

Here we briefly explain formula (24) and obtain the function $B(t)$ to calculate (27). The derivative relation can be shown simply from the fact that the anticommutator of the edge-operator with itself is proportional to the identity, i.e.

$$\{\chi_0(t), \chi_0(t')\} = 2B(t - t') \mathbb{1}, \quad (\text{D1})$$

at any time-separation. This follows from the fact that we expressed it as a linear combination of fermionic modes whose anticommutators all have the abovementioned property. The Krylov basis o_j may be generated via differentiation $o_j(t) = (2i)^{-j} \frac{d^j}{dt^j} \chi_0(t)$ of the time-evolved χ_0 , which means that

$$h_1(t) = b_1^{-1} o_1(t) \chi_0(t) = \frac{1}{2ib_1} \dot{\chi}_0(t) \chi_0(t), \quad (\text{D2})$$

where the dot denotes the time derivative. The correlator of h_1 is then the trace

$$D(t) = -\frac{1}{4b_1^2} \text{Tr}(\dot{\chi}_0(t) \chi_0(t) \dot{\chi}_0(0) \chi_0(0)), \quad (\text{D3})$$

where by Wick's theorem we have 3 different contractions among the χ_0 -s. Each of them may be expressed via the function $B(t)$ and its derivatives due to time-translation invariance, and in the end one arrives at the formula

$$D(t) = -\frac{1}{4b_1^2} \left(\dot{B}^2(0) - \dot{B}^2(t) + B(t) \ddot{B}(t) \right), \quad (\text{D4})$$

however as we will immediately see below, it turns out that $\dot{B}(0) = 0$. We calculate $B(t)$ using the fermionic mode expansion of χ_0 , that leads to an even function of t :

$$\begin{aligned} B(t) &= \text{Tr}(\chi_0(t) \chi_0(0)) / \text{Tr}(\mathbb{1}) \\ &= \sum_{k=-S}^S 2^{\delta_{k,0}-1} e^{i2\varepsilon_k t} C_k C_{-k} = \sum_{k=0}^S C_k^2 \cos(2\varepsilon_k t), \end{aligned} \quad (\text{D5})$$

which after substitution into (D4) may be reformulated as (27). Following the above steps, we can compute each correlator of the Krylov-basis elements $o_j(t)$ from $B(t)$ by differentiation.

Appendix E: Thermodynamic limit in the homogeneous chain

In this section we derive $B(t)$ for $M \rightarrow \infty$ and uniform couplings $b_m = 1$ and extract its large- t asymptotics. The structure of the latter then leads to the scaling (30) of $D(t)$.

First, let us remark on the behaviour of the fermion energies in TDL. In appendix C of [16] the dispersion relation of the uniform model

$$\varepsilon^2(p) = \frac{\sin^3 p}{\sin(p/3) \sin^2(2p/3)}, \quad p \in [0, \pi] \quad (\text{E1})$$

was derived (see Figure 6), and it was also argued in [17] that in the large M limit the solutions of $P_M(x_k = \varepsilon^{-2}(p_k)) = 0$, $M \in 3\mathbb{N}$ occupy the above interval in terms of the momentum variable p in an equidistant way $p_{k+1} - p_k \sim 3\pi/M$. The interpretation of the variable p as a lattice momentum was not explicitly given in the previous works. Such an interpretation can be given by the explicit real space representation of the fermionic operators; this computation will be presented elsewhere.

The formula above gives the supremum of the energy (thus the infimum of the roots) at $p = 0$ as

$$\frac{3\sqrt{3}}{2} > \varepsilon_k > 0, \quad x_{\text{inf}} \equiv \frac{4}{27} < x_k < \infty. \quad (\text{E2})$$

We then analyze $B(t)$ and start from finite system sizes. By looking at (D5) and the forms of the C_j coefficients in (B9) and (B17) one may realize that it is possible to rewrite the finite sum as a contour integral

$$B(t) = \frac{1}{2\pi i} \int_C dz \cos(2t/\sqrt{z}) \left(\frac{P_{M \setminus 1}(z)}{-z P_M(z)} \right), \quad (\text{E3})$$

with a keyhole contour C surrounding the half-infinite line starting from $z = x_{\text{inf}}$ as shown on the left of Figure 5. The zeros x_k of $P_M(z)$ in the denominator of the integrand introduce poles along this line, whose residues get picked up by the contour C and they are exactly the

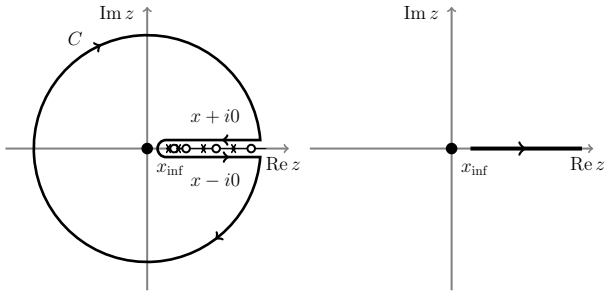


Figure 5. The contour C for integration in (E3) and the analytic structure of the integrand (left). The poles (crosses) of $P_M(x)$ and the zeros (small circles) of $P_{M \setminus 1}(x)$ thought to “condense” into the branchcut (thick line on the right) of $d(z)$ starting from x_{inf} in the $M \rightarrow \infty$ limit. The large circle picks up the residue at infinity, which gives the contribution of the zero mode. In the TDL the latter can be dropped and the rest of the contour integrates the discontinuity. For $t > 0$ the integrand has an essential singularity (black dot) at $z = 0$, while for $t = 0$ it is only a simple pole due to the factor $(-z)^{-1}$, with residue one, giving us the sum rule $\sum_{k=0}^S C_k^2 = 1$.

same as the terms under the sum in (D5). The C_0^2 term in $B(t)$ gets reconstructed by the residue at infinity

$$\begin{aligned} \text{Res}_{z=\infty} \left(\frac{\cos(2t/\sqrt{z}) P_{M \setminus 1}(z)}{-z P_M(z)} \right) & \quad (w = 1/z) \quad (\text{E4}) \\ = \text{Res}_{w=0} \left(\frac{\cos(2t\sqrt{w}) P_{M \setminus 1}(1/w)}{w P_M(1/w)} \right) & = \lim_{z \rightarrow \infty} \frac{P_{M \setminus 1}(z)}{P_M(z)}, \end{aligned}$$

that gets picked up by the large circle part of the contour. In fact, for the uniform case $b_m = 1$, this latter contribution of the zero mode always vanishes in the $M \rightarrow \infty$ limit

$$C_0^2 = \frac{3(r-1)}{M+2r} = \mathcal{O}(1/M), \quad M \in 3\mathbb{N} + r, \quad r = 1, 2, 3 \quad (\text{E5})$$

as can be easily seen from the explicit expression of the polynomials that can be found in [17].

Now we turn our attention to the $M \rightarrow \infty$ limit of the integral above. For our later convenience we introduce the rational function

$$d_M(z) \equiv \frac{P_{M \setminus 1}(z)}{P_M(z)}. \quad (\text{E6})$$

In the uniform case, where $P_{M \setminus 1}(x) = P_{M-1}(x)$, we may rewrite the recursion (12) in terms of this object as

$$1 = d_M(x) - x d_M(x) d_{M-1}(x) d_{M-2}(x) \quad (\text{E7})$$

If for a certain x there exists the limit

$$d(x) \equiv \lim_{M \rightarrow \infty} d_M(x), \quad (\text{E8})$$

then (E7) implies that the limiting value $d(x)$ has to satisfy the cubic equation

$$1 = d(x) - x d^3(x). \quad (\text{E9})$$

It follows from the definition (E6) and the behaviour of the polynomials that for large M the function $d(z)$ will have a large number of zeroes and poles at the real line for $z > 4/27$. This implies that $d_M(z)$ can not converge for these values of z . Numerical experiments confirm this expectation. On the other hand, numerical investigations show that the recursion (E7) is convergent for $\text{Im}(z) \neq 0$, $\text{Re}(z) > 0$, and the limiting value is always given by one of the roots of (E9). More concretely, we find that

$$d(z) = \begin{cases} d^{(+)}(z) & \text{Im } z > 0 \\ d^{(-)}(z) & \text{Im } z < 0 \end{cases} \quad (\text{E10})$$

where the two roots are

$$d^{(\pm)}(z) = e^{\pm i \frac{\pi}{3}} W^{\frac{1}{3}}(z) + \frac{e^{\mp i \frac{\pi}{3}}}{3z W^{\frac{1}{3}}(z)}, \quad (\text{E11})$$

and we introduced

$$W(z) \equiv \frac{1}{2z} \left(1 + \sqrt{1 - \frac{x_{\text{inf}}}{z}} \right). \quad (\text{E12})$$

When evaluated close to the positive real line as $d^{(\pm)}(x \pm i0)$, $x \in \mathbb{R}^+$, the behaviour of these two roots switches at $x = x_{\text{inf}}$ where the discriminant of the cubic equation (E9) changes sign: for $x < x_{\text{inf}}$ they both tend to the same real value, whereas for $x > x_{\text{inf}}$ they are nothing but the pair of complex conjugate roots, with a finite imaginary value. Therefore, $d(z)$ has a branchcut starting at x_{inf} , which runs along the real line into $x = +\infty$.

Let us now return to the contour integral (E3). Performing the integral surrounding the branchcut we need to evaluate the discontinuity

$$\begin{aligned} \text{Disc } d(x) &= \frac{1}{2\pi i} \left(d^{(-)}(x - i0) - d^{(+)}(x + i0) \right) \\ &= -\frac{\sqrt{3}}{2\pi} \left(W^{\frac{1}{3}}(x) - \frac{1}{3x W^{\frac{1}{3}}(x)} \right). \end{aligned} \quad (\text{E13})$$

Due to (E5) we may drop the large circle from the contour integral, thus we find

$$B(t) = \int_{x_{\text{inf}}}^{\infty} dx \frac{\cos(2t/\sqrt{x}) \text{Disc } d(x)}{(-x)}. \quad (\text{E14})$$

By the correspondence $x = \varepsilon^{-2}$ this is essentially an integral in terms of the inverse squared energy. By a change of variables via (E1) it may be rewritten as a momentum integral

$$B(t) = \int_0^{\pi} dp C^2(p) \cos(2t\varepsilon(p)), \quad (\text{E15})$$

where the function $C^2(p)$ is given by

$$\begin{aligned} C^2(p) &= -\frac{3}{2\pi} \frac{d\varepsilon^{2/3}}{dp} \left\{ \left(\varepsilon(0) + \sqrt{\varepsilon^2(0) - \varepsilon^2(p)} \right)^{1/3} \right. \\ &\quad \left. - \left(\varepsilon(0) - \sqrt{\varepsilon^2(0) - \varepsilon^2(p)} \right)^{1/3} \right\}, \end{aligned} \quad (\text{E16})$$

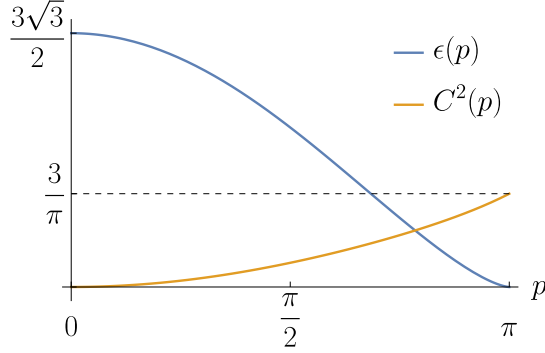


Figure 6. Behaviour of the dispersion relation $\epsilon(p)$ and the function $C^2(p)$

as expressed in terms of the dispersion relation (see Figure 6).

We also found alternative representations of the same function $B(t)$. Without derivations we communicate that it can be written also as the expansion

$$B(t) = \sum_{k=0}^{\infty} \frac{(3k)!}{k!(2k+1)!(2k)!} (-4t^2)^k \quad (\text{E17})$$

that is equivalent to the special function (29). Detailed derivations of this alternative representation, together with connections to the combinatorical properties of the recursion (E7) will be presented elsewhere.

Appendix F: Long time asymptotics

The integral (E15) is an exact representation of (29). Here we extract its large time asymptotics, using the stationary phase approximation. The stationary points of the energy are exactly at the lowest and highest momentum, and the energy and the function $C^2(p)$ behaves as

$$\varepsilon(p) = \begin{cases} \varepsilon(0) \left(1 - \frac{1}{6}p^2 + \mathcal{O}(p^4)\right) \\ \left(\frac{4}{3}\right)^{3/4} |\pi - p|^{3/2} + \mathcal{O}(|\pi - p|^{5/2}) \end{cases} \quad (\text{F1})$$

and

$$C^2(p) = \begin{cases} \frac{p^2}{3\pi} + \mathcal{O}(p^4) & p \simeq 0 \\ \frac{3}{\pi} + \mathcal{O}(|\pi - p|) & p \simeq \pi \end{cases} \quad (\text{F2})$$

respectively around these points, see also Figure 6. In the first case, at $p \simeq 0$ we have to evaluate (properly regulated) complex Gaussian integrals that give

$$\begin{aligned} \frac{1}{4} \sum_{\sigma=\pm} \int_{-\infty}^{\infty} dp \frac{p^2}{3\pi} e^{i\sigma 2\varepsilon(0)(1-\frac{1}{6}p^2)} \\ = -\sqrt{\frac{3}{2\pi}} \frac{\sin(2\varepsilon(0)t + 3\pi/4)}{(2\varepsilon(0)t)^{3/2}}, \end{aligned} \quad (\text{F3})$$

for $t > 0$, whereas for $p \simeq \pi$, after changing variables to $\eta = \left(\frac{4}{3}\right)^{3/4} |\pi - p|^{3/2}$ we get

$$\begin{aligned} \frac{1}{2} \sum_{\sigma=\pm} \int_{-\infty}^{\pi} dp \frac{3}{\pi} e^{i\sigma 2t(4/3)^{3/4} |\pi - p|^{3/2}} \\ = \frac{1}{2} \sum_{\sigma=\pm} \int_0^{\infty} d\eta \frac{\sqrt{3}}{\pi} \eta^{-1/3} e^{i\sigma 2t\eta} = \frac{\sqrt{3}\Gamma(\frac{2}{3})}{2\pi \times (2t)^{2/3}}. \end{aligned} \quad (\text{F4})$$

Although we could continue these approximations around the two stationary points, and both would give a family of corrections to $B(t)$ as inverse fractional powers of t competing in magnitude, we stop at the lowest order terms derived above

$$B(t) \sim \frac{B_{\pi}}{t^{2/3}} + \frac{B_0(t)}{t^{3/2}}. \quad (\text{F5})$$

Here we indicated their structure with the constant B_{π} and the oscillating function $B_0(t)$ that can be read off from the r.h.s. of (F4) and (F3) respectively. Substituting this into (24) tells us that the leading term in the correlator of h_1 should behave with t to the inverse power with exponent $2/3 + 3/2 = 13/6$, more precisely as

$$D(t) \sim -\frac{B_{\pi} \ddot{B}_0(t)}{4t^{13/6}} = -\frac{3 \times 3^{3/4} \Gamma(\frac{2}{3})}{16 \times 2^{1/6} \pi^{3/2}} \frac{\sin(2\varepsilon(0)t + 3\pi/4)}{t^{13/6}}, \quad (\text{F6})$$

fixing the constant $\alpha \approx -0.0926$ in (30).

Appendix G: Floquet time evolution from the transfer matrix

As it was described in the main text, the transfer matrix admits a factorization into a product of local gates, such that for purely imaginary rapidities we obtain a unitary quantum circuit. More precisely, the transfer matrix becomes an operator that is proportional to a unitary quantum circuit. In the present conventions we get

$$\mathcal{V}(\delta) = \frac{T_M(-i\delta)}{\sqrt{P_M(-\delta^2)}}. \quad (\text{G1})$$

Here we obtained the additional normalization factor from the inversion relation (11).

The transfer matrix can be written [16] via the $\Psi_{k \neq 0}$ operators as

$$T_M(u) = \prod_{k=1}^S \left(1 - \frac{u}{u_k} [\Psi_k, \Psi_{-k}] \right). \quad (\text{G2})$$

Then, using solely (B16), a conjugation with the transfer matrix for $k \neq 0$

$$\frac{T_M(u) \Psi_k T_M(-u)}{P_M(u^2)} = \frac{u_k - u}{u_k + u} \Psi_k \quad (\text{G3})$$

will only introduce the above prefactor, where for negative k -s $u_{-|k|} \equiv -u_{|k|}$ is understood. After analytic continuation $u \rightarrow -i\delta$ this turns into a phase

$$\frac{u_k + i\delta}{u_k - i\delta} = e^{i2\arctan(\varepsilon_k\delta)}. \quad (\text{G4})$$

Then, several unitaries will act as

$$\mathcal{V}^N(\delta)\Psi_k\mathcal{V}^N(-\delta) = e^{i\theta_k}\Psi_k, \quad \theta_k = 2N\arctan(\varepsilon_k\delta). \quad (\text{G5})$$

For the $k = 0$ zero mode we have $\theta_0 = 0$, as the conjugation on the l.h.s. of (G3) leaves Ψ_0 invariant.

At this point we have to perform very similar steps to what we had in Section E to calculate the two-point function of h_1 with itself. That is, substitute (22) into (33) and evolve the product of two fermions via (G5). After that, taking the trace leads to the the same structure, the only difference is that now one needs to compute the traces of four fermion terms directly. However, this is straightforward and it leads to the same formula, and only the phases θ_k are modified.

Appendix H: Factorization of the 3-site gate

Here we provide an explicit factorization of the gates in the quantum circuit described in the main text. The circuit (31) consists of 3-site gates

$$u_j \equiv \exp(i\varphi_j h_j) = \exp(i\varphi_j Z_{j-2}Z_{j-1}X_j). \quad (\text{H1})$$

After expanding the exponential in the definition, the gate simply looks as

$$u_j = \cos \varphi_j + i \sin \varphi_j Z_{j-2}Z_{j-1}X_j. \quad (\text{H2})$$

Based on the idea of uniformly controlled unitaries in [39] we express this operator as a product of quantum gates.

As the rotations in (H2) are around the x -axis, the set of gates we use is such a 1-qubit rotation

$$[R_X(\varphi)]_j = e^{i\frac{\varphi}{2}X_j} = \cos \frac{\varphi}{2} + i \sin \frac{\varphi}{2} X_j \quad (\text{H3})$$

and controlled-Y, or CY gates:

$$[\text{CY}]_{k,l} = e^{i\frac{\pi}{4}(\mathbb{1}-Z_k)(\mathbb{1}-Y_l)} = \frac{1}{2} (1 + Z_k + Y_l - Z_k Y_l), \quad (\text{H4})$$

where k is the control qubit and l is the controlled one. The square of the CY gate is the identity, and inserting an X operator on the controlled qubit between two such gate gives $[\text{CY}]_{k,j}X_j[\text{CY}]_{k,j} = Z_k X_j$ for $k \neq j$. This leads to the idea to represent u_j by conjugating the rotation operator on the j^{th} site twice, by two different CY gates. In fact we obtain the factorization (see Figure 2):

$$u_j = [\text{CY}]_{j-2,j}[\text{CY}]_{j-1,j}[R_X(2\varphi_j)]_j[\text{CY}]_{j-1,j}[\text{CY}]_{j-2,j}. \quad (\text{H5})$$

Close to the boundary of the system, i.e. for $j = 1, 2$ the CY gates whose control bit would lie outside the index range $1, 2, \dots, M$ should be replaced by an identity in formula (H5), as can be seen in Figure 3.

Appendix I: Comparison with exact diagonalization

To show how much more powerful the analytical method is than numerical exact diagonalization (ED) we plot the analytical results for the energy-energy correlation function (27) against those given by ED (see Fig. 7). Much higher system sizes can be reached analytically than using numerical ED on a desktop PC. The difficulty that limits the evaluation of the analytical formula (27) is finding all the roots of the polynomial $P_M(x)$ (12). The order of the polynomial grows as $S = [(M+2)/3]$ and thus for large M it becomes difficult to find the roots. Using the NSolve function of Mathematica we can go up to $M = 60$. Meanwhile, the largest system size reachable by numerical ED on an average desktop PC without parallelization is $M = 12$.

[1] T. D. Schultz, D. C. Mattis, and E. H. Lieb, Two-dimensional ising model as a soluble problem of many fermions, *Rev. Mod. Phys.* **36**, 856 (1964).

[2] E. Lieb, T. Schultz, and D. Mattis, Two soluble models of an antiferromagnetic chain, *Ann. Phys.* **16**, 407 (1961).

[3] A. Y. Kitaev, Unpaired majorana fermions in quantum wires, *Physics-Uspekhi* **44**, 131 (2001).

[4] A. Kitaev, Anyons in an exactly solved model and beyond, *Ann. Phys.* **321**, 2 (2006), arXiv:cond-mat/0506438 [cond-mat.mes-hall].

[5] L. G. Valiant, Quantum circuits that can be simulated classically in polynomial time, *SIAM Journal on Computing* **31**, 1229 (2002).

[6] B. M. Terhal and D. P. Divincenzo, Classical simulation of noninteracting-fermion quantum circuits, *Phys. Rev. A* **65**, 032325 (2002), arXiv:quant-ph/0108010 [quant-ph].

[7] R. Jozsa and A. Miyake, Matchgates and classical simulation of quantum circuits, *Proc. Roy. Soc. Lond. A* **464**, 3089 (2008), arXiv:0804.4050 [quant-ph].

[8] A. Jahn and J. Eisert, Holographic tensor network models and quantum error correction: a topical review, *Quantum Sci. Tech.* **6**, 033002 (2021), arXiv:2102.02619 [quant-ph].

[9] P. Jordan and E. Wigner, Über das paulische äquivalenzverbot, *Z. Physik* **47**, 631 (1928).

[10] K. Minami, Solvable Hamiltonians and Fermionization Transformations Obtained from Operators Satisfying Specific Commutation Relations, *J. Phys. Soc. Japan* **85**, 024003 (2016).

[11] K. Minami, Infinite number of solvable generalizations of XY-chain, with cluster state, and with central charge $c = m/2$, *Nucl. Phys. B* **925**, 144 (2017), arXiv:1710.01851

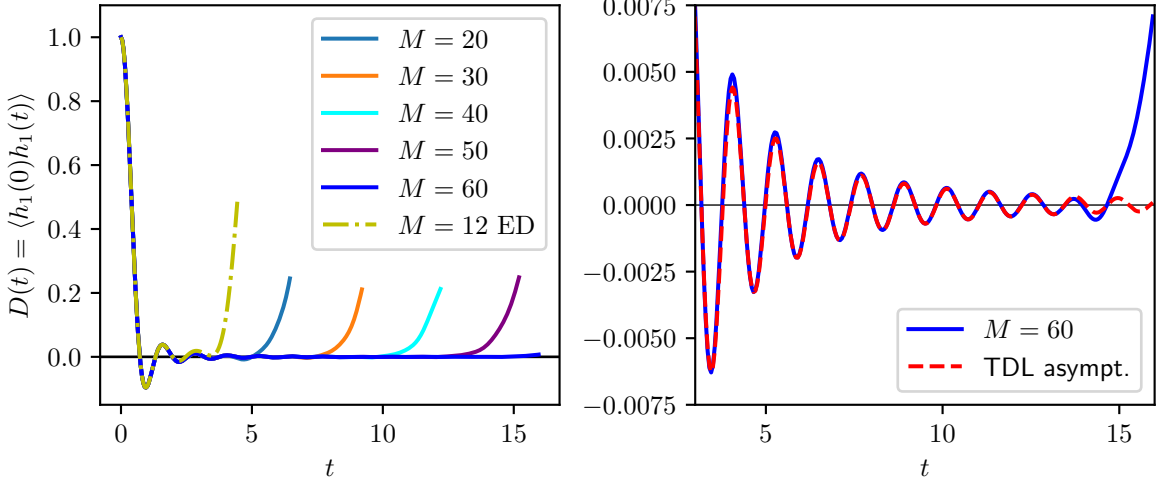


Figure 7. Left: the dashed-dotted line shows the numerical exact diagonalization result for the energy-energy correlation function at the largest reasonable system size for an average desktop PC without parallelization ($M = 12$). Full lines show the analytical result (27) for the energy-energy correlation function at different system sizes M . Right: comparison of the asymptotics of the analytical result at $M = 60$ with the asymptotics in the thermodynamic limit (30).

[cond-mat.stat-mech].

- [12] Y. Yanagihara and K. Minami, Exact solution of a cluster model with next-nearest-neighbor interaction, *Progr. of Theor. Exp. Phys.* **2020**, 113A01 (2020), arXiv:2003.00962 [cond-mat.stat-mech].
- [13] M. Ogura, Y. Imamura, N. Kameyama, K. Minami, and M. Sato, Geometric criterion for solvability of lattice spin systems, *Phys. Rev. B* **102**, 245118 (2020), arXiv:2003.13264 [cond-mat.stat-mech].
- [14] A. Chapman and S. T. Flammia, Characterization of solvable spin models via graph invariants, *Quantum* **4**, 278 (2020), arXiv:2003.05465 [quant-ph].
- [15] Z. Wang and K. R. A. Hazzard, Particle exchange statistics beyond fermions and bosons, *Nature* **637**, 314 (2025), arXiv:2308.05203 [quant-ph].
- [16] P. Fendley, Free fermions in disguise, *J. Phys. A* **52**, 335002 (2019), arXiv:1901.08078 [cond-mat.stat-mech].
- [17] F. C. Alcaraz and R. A. Pimenta, Free fermionic and parafermionic quantum spin chains with multi-spin interactions, *Phys. Rev. B* **102**, 121101 (2020), arXiv:2005.14622 [cond-mat.stat-mech].
- [18] F. C. Alcaraz and R. A. Pimenta, Integrable quantum spin chains with free fermionic and parafermionic spectrum, *Phys. Rev. B* **102**, 235170 (2020), arXiv:2010.01116 [cond-mat.stat-mech].
- [19] S. J. Elman, A. Chapman, and S. T. Flammia, Free fermions behind the disguise, *Commun. Math. Phys.* **388**, 969 (2021), arXiv:2012.07857 [quant-ph].
- [20] A. Chapman, S. J. Elman, and R. L. Mann, A Unified Graph-Theoretic Framework for Free-Fermion Solvability, arXiv e-prints , arXiv:2305.15625 (2023), arXiv:2305.15625 [quant-ph].
- [21] P. Fendley and B. Pozsgay, Free fermions beyond Jordan and Wigner, *SciPost Physics* **16**, 102 (2024), arXiv:2310.19897 [cond-mat.stat-mech].
- [22] P. Fendley and K. Schoutens, Cooper pairs and exclusion statistics from coupled free-fermion chains, *J. Stat. Mech.* **2007**, 02017 (2007), arXiv:cond-mat/0612270 [cond-mat.stat-mech].
- [23] J. de Gier, G. Z. Feher, B. Nienhuis, and M. Rusaczonek, Integrable supersymmetric chain without particle conservation, *J. Stat. Mech.* , 023104 (2016), arXiv:1510.02520 [cond-mat.quant-gas].
- [24] G. Z. Feher, A. Garbali, J. de Gier, and K. Schoutens, A curious mapping between supersymmetric quantum chains, in *2017 MATRIX Annals* (Springer International Publishing, Cham, 2019) pp. 167–184, arXiv:1710.02658 [cond-mat.stat-mech].
- [25] F. C. Alcaraz and R. A. Pimenta, Free-parafermionic $z(n)$ and free-fermionic xy quantum chains, *Phys. Rev. E* **104**, 054121 (2021), arXiv:2108.04372 [cond-mat.stat-mech].
- [26] F. C. Alcaraz, J. A. Hoyos, and R. A. Pimenta, Powerful method to evaluate the mass gaps of free-particle quantum critical systems, *Phys. Rev. B* **104**, 174206 (2021), arXiv:2109.01938 [cond-mat.stat-mech].
- [27] F. C. Alcaraz, R. A. Pimenta, and J. Sirker, Ising analogs of quantum spin chains with multi-spin interactions, *Phys. Rev. B* **107**, 235136 (2023), arXiv:2303.15284 [cond-mat.stat-mech].
- [28] F. C. Alcaraz, J. A. Hoyos, and R. A. Pimenta, Random free-fermion quantum spin chain with multi-spin interactions, *Phys. Rev. B* **108**, 214413 (2023), arXiv:2308.16249 [cond-mat.dis-nn].
- [29] A. Chapman, S. T. Flammia, and A. J. Kollár, Free-Fermion Subsystem Codes, *PRX Quantum* **3**, 030321 (2022), arXiv:2201.07254 [quant-ph].
- [30] B. Pozsgay, Quantum circuits with free fermions in disguise, arXiv e-prints (2024), arXiv:2402.02984 [quant-ph].
- [31] P. Fendley, Free parafermions, *J. Phys. A* **47**, 075001 (2014), arXiv:1310.6049 [cond-mat.stat-mech].
- [32] K. Tran, Connections between discriminants and the root distribution of polynomials with rational generating function, *J. Math. An. Appl.* **410**, 330 (2014), arXiv:1601.04382 [math.CV].

- [33] T. Forgács and K. Tran, On the zeros of polynomials generated by rational functions with a hyperbolic polynomial type denominator, *Constr. Approx.* **46**, 617 (2017), [arXiv:1606.07125 \[math.CV\]](https://arxiv.org/abs/1606.07125).
- [34] J.-P. Allouche and T. Johnson, Narayana's Cows and Delayed Morphisms, in *Journées d'Informatique Musicale* (île de Tatihou, France, 1996).
- [35] O. F. I. (2024), Entry a000930 in the on-line encyclopedia of integer sequences, <https://oeis.org/A000930>.
- [36] J. Stolze, V. Viswanath, and G. Müller, Dynamics of semi-infinite quantum spin chains at $t = \infty$, *Z. Physik B* **89**, 45 (1992).
- [37] I. S. Eliëns, F. B. Ramos, J. C. Xavier, and R. G. Pereira, Boundary versus bulk behavior of time-dependent correlation functions in one-dimensional quantum systems, *Phys. Rev. B* **93**, 195129 (2016), [arXiv:1602.01679 \[cond-mat.str-el\]](https://arxiv.org/abs/1602.01679).
- [38] U. Javed, J. Marino, V. Oganesyan, and M. Kolodrubetz, Counting edge modes via dynamics of boundary spin impurities, *Phys. Rev. B* **108**, L140301 (2023), [arXiv:2111.11428 \[cond-mat.stat-mech\]](https://arxiv.org/abs/2111.11428).
- [39] M. Möttönen, J. J. Vartiainen, V. Bergholm, and M. M. Salomaa, Quantum Circuits for General Multiqubit Gates, *Phys. Rev. Lett.* **93**, 130502 (2004), [arXiv:quant-ph/0404089 \[quant-ph\]](https://arxiv.org/abs/quant-ph/0404089).